

Effect of surfactant type on the microstructure and optical properties of In_2O_3 nanoparticles

KANICA ANAND, PRAVEEN KUMAR, R. THANGARAJ*

Semiconductors Laboratory, Department of Physics, GND University, Amritsar-143005, India

This paper reports the sol-precipitation synthesis of spherical In_2O_3 nanoparticles. The effect of the use of different surfactants on the growth, microstructure and optical properties has been studied. The lattice parameter for cubic crystalline nanoparticles from the diffraction data and strain and crystallite size have been calculated by using the Williamson-Hall plots. The blue shift in the absorption edge and two characteristic luminescence bands for PVP and CPC grown samples have been observed. The change in the optical and luminescence behavior of the nanoparticles has been attributed to the effect of precursors used which controls the growth/microstructure along with the size of the nanoparticles.

(Received April 12, 2011; accepted June 9, 2011)

Keywords: In_2O_3 nanoparticles, Microstructure, Optical and luminescence properties

1. Introduction

Semiconductor nanostructures have been attracting increasing attention because of their exceptional properties, which differ from those of their bulk counterparts, and because of their potential application in optoelectronic devices. They exhibit many interesting novel size- and shape-dependent properties based on which it is extensively used in the design of solar cells, UV lasers and light emitting diodes, window heaters, flat panel displays, and photocatalysts. Potential applications have been explored in the recent past. In particular, the indium oxide is n-type semiconductor with a wide band gap (3.6eV), giving high transparency suitable for many solid state devices [1-5]. Its thin/thick films are also well characterized for the gas sensing applications due to the increase in the surface to volume ratio for the nanostructures giving large value of the response as well as the selectivity for different gasses [6]. However, many approaches both physical and chemical ones have been developed for controlling the size, shape and surface characteristics, but the control of the point, external surface and volume defects have been frozen in the nanocrystals, which not only influences the intrinsic properties but also effects the long time stability or response characteristics as well as luminescence properties of the solid state devices [1-6]. Various new approaches are required to control the growth of nano-particles, where, these intrinsic defects could be eliminated or their effect be minimized. The use of different polymers has resulted in the control of the growth, shape of the nanostructures with the improvement of the physical properties [7]. Therefore, the present work reports the effect of the surfactant type on the growth of microstructure, optical

and photoluminescence properties of sol-precipitation synthesized In_2O_3 nanoparticles.

2. Experimental details

Indium nitrate ($\text{In}(\text{NO}_3)_3 \cdot \text{H}_2\text{O}$, CDH), citric acid (CA, MW=192.1gm/mol, Thomas Baker), Urea ($(\text{NH}_2)_2\text{CO}$, Thomas Baker), Poly(vinyl pyrrolidone) (PVP, MW=55000gm/mol, Sigma Aldrich) and cationic cetylpyridinium chloride (CPC, MW=358.01gm/mol, Sigma Aldrich) were used without any additional purification in the present work. In a typical experimental procedure for the synthesis of precursor $\text{In}(\text{OH})_3$ nanoparticles, three different solutions: 0.2M solution was prepared by dissolving $\text{In}(\text{NO}_3)_3 \cdot \text{H}_2\text{O}$ (1.275g) with rigorous stirring for 3h at room temperature, 0.1M solution of CA (0.384g) and 1.5M urea solution (1.8g) have been separately made in 20ml de-ionized water. The precursor ratio taken in the present study has reported to yield low polydisparsity with spherical size of the nanoparticles [3]. Then, all the three solutions were mixed together and reaction takes place at 90°C for 3h with the formation of white precipitates. These particles were firstly filtered, then washed with ethanol several times and finely dried at 105°C for half hour. Similarly, the surfactant solution (0.012gm for PVP and 0.034g for CPC prepared in 4ml of de-ionized water) was mixed properly with the precursor solution and following the same procedure.

The transformation of the precursor particles into In_2O_3 nanoparticles, the calcinations at 250°C for 12h results in the amorphous particles while 500°C for 2h results in the formation of crystalline cubic In_2O_3 nanoparticles. The different nano-particles was characterized by x-ray diffraction (D8 Focus, Bruker,

Germany) technique using Cu K_α radiation ($\lambda=0.154\text{nm}$) at 40kV and 20mA power conditions. FTIR spectroscopic studies from 4000-400cm⁻¹ have been performed using the KBr pallet method (1100, Shimadzu, Japan) The optical absorption spectra for the nanoparticles/ethanol solution by using the spectrophotometer (Lambda 35, Perkin Elmer, USA) and photoluminescence studies using the fluorescence spectrophotometer (Lambda 45, Perkin Elmer, USA) at 290nm excitation.

3. Results and Discussion

3.1 Growth and Microstructure

Fig. 1 shows the XRD patterns of the as synthesized precipitates shows the diffraction peak at 22.4° for the cubic In(OH)₃ nanoparticles. The analysis of the diffraction data for the calculation of different parameters was performed using the PowderX software [8]. The particle size has been calculated by using the Debye Scherrer's equation ($D=0.89\lambda/(\beta \cos\theta)$), where λ , θ and β are the x-ray wavelength, diffraction angle and full width at half maximum of the high intensity peak respectively. The crystallite size varies as 13.4nm, 11.8nm and 10.3nm for without surfactant, PVP and CPC respectively. IR absorption spectrum shows the absorption bands for In-OH (1087.1cm⁻¹), In-O (526.1cm⁻¹) for all the three samples (IR absorption spectra are not shown here). No signature for surface passivation occurs in the formation of precursor In(OH)₃ nanoparticles with the absence of the signature bands (in the present case PVP, CPC) from the IR studies. It is therefore understood that the use of surfactant may affect the growth/morphology of the nanoparticles and does not form the capping layer on the nanoparticles. The annealing of these nanoparticles at 250°C for 12h results in the formation of amorphous In₂O₃ nanoparticles (no sharp diffraction peaks) while the annealing at 500°C for 2h results in the formation of crystalline In₂O₃ nanoparticles. Fig. 1 show the diffraction scans for all the three samples made and all the diffraction peaks were indexed by using the JCPDS 06-416 file. It has been observed that the high intensity for the (222) peak (crystallite size~18.9nm), while (211), (400), (440) and (622) are the other diffraction peaks for In₂O₃ nanoparticles. It has been observed that using PVP surfactant, the diffraction peak for (222) phase shifts towards higher 2 θ -values while at lower angles for CPC grown nanoparticles. The addition of the surfactant leads to a relative change in the intensity and/or fwhm of different diffraction peaks. The particle size for all the samples is ~18.9nm and the lattice parameter calculated using the (222) diffraction peak are summarized in Table 1. Similar value of the lattice parameter has been reported elsewhere [1], while its value decreases with PVP, while an increase for the CPC used samples has been observed.

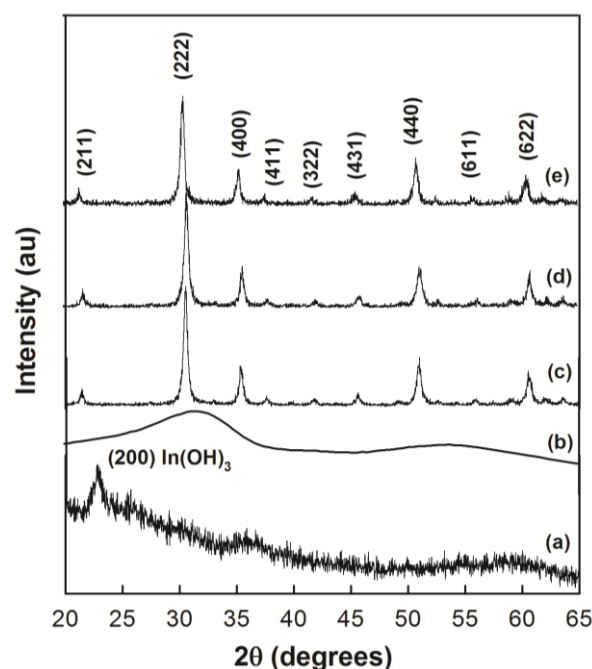


Fig. 1. X-ray diffraction patterns for the (a) as-synthesized In(OH)₃ nanoparticles, calcined powders at (b) 250°C for 3h without surfactant, and others (c) without surfactant, (d) PVP and (e) CPC used In₂O₃ nanoparticles calcined at 500°C for 1h respectively.

Table 1: Summarization of the different calculated and observed parameters for synthesized In₂O₃ nanoparticles.

Sample	a (Å)	ϵ (nm)	$\eta (\times 10^{-3})$	PL peak (nm)		E _o (eV)
				1	2	
In ₂ O ₃ :Pure	10.14	22.6	+1.6±0.3	432	484	3.70
In ₂ O ₃ :PVP	10.06	18.1	-1.6±1.2	440	482	3.92
In ₂ O ₃ :CPC	10.16	33.5	+8.5±2.5	430	468	3.83

The line broadening and the peak shift observed for the (222) peak for the nanoparticles grown differently can be ascribed due to the simultaneous size and strain effects [9]. Therefore, it is interesting to properly correlate the role of surfactant on the growth parameters or separate the different contributions due to strain and crystallite size of the nanoparticles considering four different peaks by using the Williamson-Hall equation: $\beta \cos\theta = 1/\epsilon + \eta \sin\theta/\lambda$, where λ is the X-ray wavelength, β is the full width at half maximum (fwhm), θ is the Bragg's diffraction angle, ϵ is the effective particle size and η is the effective microstrain respectively. The plots of $\beta \cos\theta/\lambda$ versus $\sin\theta/\lambda$, may have positive slopes tells about the presence of tensile strain for large grain size samples while the negative one corresponds to the compressive strain in smaller grain size samples.

Fig. 2 shows the plot of $\beta \cos\theta/\lambda$ versus $\sin\theta/\lambda$, revealing a negative slope for each sample. From the linear fit, effective particle size and the effective strain has been calculated and summarized in Table 1. It has been observed that the negative value of stain with smaller value of particle size for the PVP used samples while positive value with larger particle size than the parent nanoparticles has been observed. The compressive strain could be due to the presence of vacancies at the lattice points due to the absence of indium ions at their lattice points with the reduction of the grain size for the particles synthesized using the polymer PVP, while for the nanoparticles synthesized using the CPC or without surfactant ones have found the tensile strain. Since PVP acts as structure directing a template during the growth [7] and simultaneous use of urea opens the entangled polymer chains giving smaller particle size with compressive strains while the micelle solution formed with the use of cationic surfactant (CPC) acts as nucleating and structure directing component giving larger particle size and larger strains in the synthesized nanoparticles.

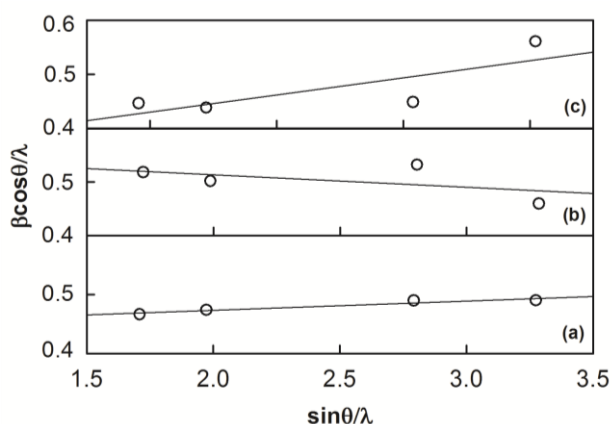


Fig. 2: Williamson-Hall plots for the (a) without, (b) PVP and (c) CPC surfactant used samples for the In_2O_3 nanoparticles respectively.

3.2 Optical and photoluminescence studies

Optical absorption and photoluminescence spectroscopy have been studied to elaborate the effect of the strain frozen growth due to the creation of different type of vacancies in the nanoparticles. Fig. 3 shows the absorbance spectra and room temperature luminescence 300nm excitation for all the nanoparticles. It has been observed that pure In_2O_3 nanoparticles exhibit a broad absorption band at 3.7 eV and with the use of PVP, it blue shifts to 3.92 eV while further change to cationic surfactant, CPC gives two absorption maxima at 3.83 eV and 3.16 eV respectively. Since the use of different surfactants during the solution based synthesis routes causes a change in the nucleation and growth kinetics resulting in the selectivity in the size, shape, morphology, phase and crystalline structure of the grown nanoparticles for a particular growth process. The changes could also be attributed to the change in the particle size as well the

intrinsic defects frozen in the nanocrystals. Although, the small value of the strain in the pure and PVP grown nanoparticles, a single absorption band observed, while the increase in the strain in CPC grown nanoparticles due to higher defects in the particles gives another dominant level in between the optical gap on the material.

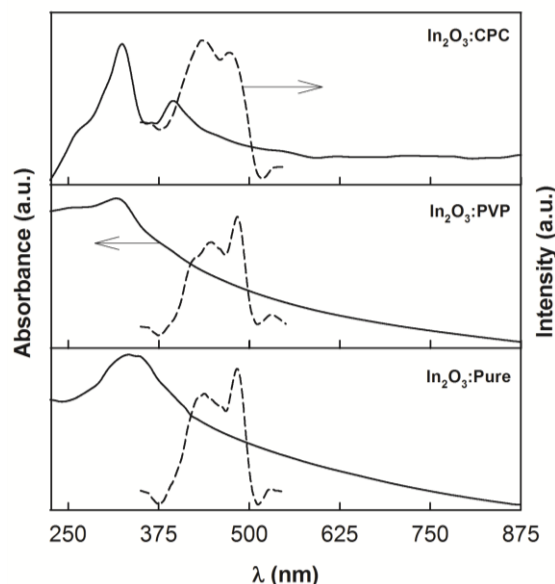


Fig. 3. Optical absorbance and photoluminescence characteristics with excitation at 300nm for In_2O_3 nanoparticles.

On the other hand, all the grown nanoparticles exhibit two luminescence bands with peak values at 432nm (I-peak) and 484nm (II-peak) in the visible region of the spectrum for pure In_2O_3 nanoparticles [2, 5]. The use of the PVP results in the red shift in the first luminescence band while the use of cationic surfactant, CPC gives an enhancement in the relative luminescence of the first peak with a slight blue shift for the second luminescence band. The formation of vacancies during the particle synthesis might result in the strained particles or enhancement in the defect state density or the new energy levels in the band gap of the semiconductor.

The blue emission has been assigned due to the radioactive recombination of a photo-excited hole with an electron occupying the oxygen vacancies and the UV emission is ascribed to the influence of the lattice defects, interstitials and high density of oxygen/indium vacancies generated because of incomplete oxidation and crystallization process [5]. Thus, the like luminescence for pure and PVP grown nanoparticles shows the similar optical transitions although the absorption edge shifts to the lower wavelengths with the use of PVP. Since, the band edge transition lies in the UV region for nanoparticles with 10-30nm size, thus, the observed luminescence could be from the mid gap states due to the defects frozen in the nanoparticles. As the particle size remains almost similar, but the change/increase in the

strain type may result in the introduction of new defects between the gap for the surfactant used samples. But, the observation additional shoulder band at 367nm due to the band edge emission due to increase in the defects for the CPC grown nanoparticles.

4. Conclusions

In the present work, we have studied the effect of different surfactants on the growth, microstructure and optical properties of the spherical In₂O₃ nanoparticles. The decrease in the particle size, lattice parameter along with a negative value of strain for the PVP used samples while an increase in both ones with CPC surfactant has been observed. The blue shift of absorption edge for the PVP and CPC grown samples have been observed. The change in the position of the two characteristic luminescence bands with the differently grown nanoparticles has been observed and attributed to the effect of precursors used which controls the growth/microstructure along with the size of the nanoparticles.

Acknowledgements

One of the authors (KA) is thankful to DST, India for providing M.Sc. Nano Science and Technology Studentship.

References

- [1] D. Chu, Y. Zeng, D. Jiang, J. Xu, *Nanotechnology* **18**, 435605 (2007)
- [2] M. J. Zheng, L. D. Zhang, G. H. Li, X. Y. Zhang, X. F. Wang, *Appl. Phys. Lett.* **79(6)**, 839 (2001)
- [3] S. Lin, W. J. Weiw, *J. Am. Ceram. Soc.* **91(4)**, 1121 (2008)
- [4] E. A. Forsha, A. V. Marikutsaa, M. N. Martyshova, P. A. Forsha, M. N. Rumyantsevaa, A. M. Gaskova, P. K. Kashkarova, *J. Exp. Th. Phys.* **111(4)**, 653 (2010)
- [5] Y. Zhao, Z. Zhang, Z. Wu, H. Dang, *Langmuir* **20**, 27 (2004)
- [6] A. Oprea, A. Gurlo, N. Barsan, U. Weimar, *Sens. Act. B: Chem.* **139(2)**, 322 (2009)
- [7] B. Panigrahy, M. Aslam, D. S. Misrab, D. Bahadur, *CrystEngComm*, **11**, 1920 (2009)
- [8] C. Dong, *J. Appl. Cryst.* **32**, 838 (1999)
- [9] M. M. Savosta, V. N. Krivoruchko, I. A. Danilenko, V. Y. Tarenkov, T.E. Konstantinova, A.V. Borodin, V.N. Varyukhin, *Phys. Rev. B* **69**, 024413 (2004)

*Corresponding author: rthangaraj@rediffmail.com